

Dynamics of vacancy-mediated phase separation

Sanjay Puri

School of Physical Sciences, Jawaharlal Nehru University, New Delhi 110067, India;
Beckman Institute, 405 N. Matthews Avenue, University of Illinois at Urbana-Champaign, Urbana, Illinois 61801-3080;
and Department of Theoretical Physics, University of Manchester, Manchester M13 9PL, United Kingdom
 (Received 28 May 1996)

We formulate a mean-field (MF) dynamical model for vacancy-mediated phase separation in ternary ABV mixtures, where A and B refer to the separating components; and V to vacancies. We use this model to obtain numerical results for the scaled structure factor and the characteristic length scale, which are then compared with results from a MF dynamical model of phase separation via the usual Kawasaki-exchange mechanism. [S1063-651X(97)15902-5]

PACS number(s): 64.75.+g, 64.60.-i

Much interest has focused on the area of phase ordering dynamics, viz., the temporal evolution of a homogeneous two-phase mixture which has been rendered thermodynamically unstable by a sudden quench below the critical temperature [1]. Typically, the evolving system separates into domains which are rich in one or the other constituent of the mixture. For pure and isotropic systems, it is well established that the coarsening domains are characterized by a unique time-dependent length scale $L(t)$, where t is the time. A consequence of this is that the time-dependent correlation function $g(\vec{r}, t)$ of the coarsening system has a trivial dependence on time in that $L(t)$ merely serves as a scale for the distance variable r , i.e., $g(\vec{r}, t) \equiv G(r/L(t))$ [2]. The physical implication of this ‘‘dynamical scaling’’ property is that the morphology of the coarsening domains is self-similar in time. Interest in this area has primarily focused on the time dependence of $L(t)$; and the functional forms of the scaled correlation function and structure factor [1]. These properties depend critically on whether the evolving system is characterized by a nonconserved order parameter (e.g., ordering of a ferromagnet); or a conserved order parameter (e.g., segregation of a binary mixture AB). There is a reasonable understanding of the nonconserved order parameter (NCOP) case at the experimental, numerical and theoretical levels. The case with conserved order parameter (COP) is also well understood experimentally and numerically. However, at the theoretical level, there is still no reliable theory which explains all features of the scaled structure factor.

A number of recent studies have focused on incorporating experimentally relevant effects into the modeling and simulation of phase ordering dynamics. An important experimental complication in two-phase mixtures is the presence of quenched and annealed disorders. In this paper, we will study the dynamics of phase separation in ternary ABV mixtures, where the third component V refers to vacancies. We have a specific motivation for this study, which is as follows. Conventional Monte Carlo (MC) studies of phase separation dynamics in ‘‘pure’’ AB alloys associate Kawasaki spin-exchange kinetics [3] with a two-state Ising model. In these models, the spin variable S_i at site i takes the value $+1$ or -1 if it is occupied by an A or B atom, respectively. Segregation proceeds via the exchange of A and B atoms on

neighboring sites. However, even though this simple dynamics has attractive features, it is microscopically unrealistic because of the extremely high energies involved. As a matter of fact, materials scientists believe that segregation in binary alloys is mediated by vacancies [4]. Thus, in the context of binary alloys, vacancies serve a crucial role in the dynamics of segregation, and should not merely be viewed as experimental complications.

These have been a number of studies of vacancy-mediated phase separation [5,6] which we briefly review here. To the best of our knowledge, this problem was first investigated by Yaldrum and Binder [5] via MC studies of a three-state spin model. They found that the vacancies tended to migrate to interfacial regions. Moreover, their results suggested that the qualitative behavior of vacancy-mediated phase separation is the same as that for the usual Kawasaki-exchange models. However, they did not make a quantitative comparison or investigate the late-stage behavior.

A more recent MC study was conducted by Fratzl and Penrose [6], who investigated phase separation in an AB mixture mediated by a single vacancy. They found that domain growth in their model is much faster than that for the usual Kawasaki-exchange model. As a matter of fact, they had no difficulty in accessing the asymptotic Lifshitz-Slyozov [$L(t) \sim t^{1/3}$] growth regime, which has not been possible so far even in the most exhaustive MC simulations of Kawasaki-exchange models [7]. We should stress here that the Fratzl-Penrose model is in the same static universality class as the usual two-state Ising model for binary mixtures. This is because a single vacancy is not relevant in the thermodynamic limit.

In this paper, we formulate mean-field (MF) dynamical models for vacancy-mediated phase separation in ABV models. We use the master equation approach [8] to obtain reasonable phenomenological models for this problem. For segregation in pure binary mixtures, coarse-grained models have proven of great utility in accessing the asymptotic behavior [9]. It is our belief that the same will be true here also. We simulate these MF dynamical models up to late times and provide detailed results for the domain growth law and the scaled structure factor.

The starting point of our modeling is a lattice model in which each site i can be occupied by either an A , B , or V

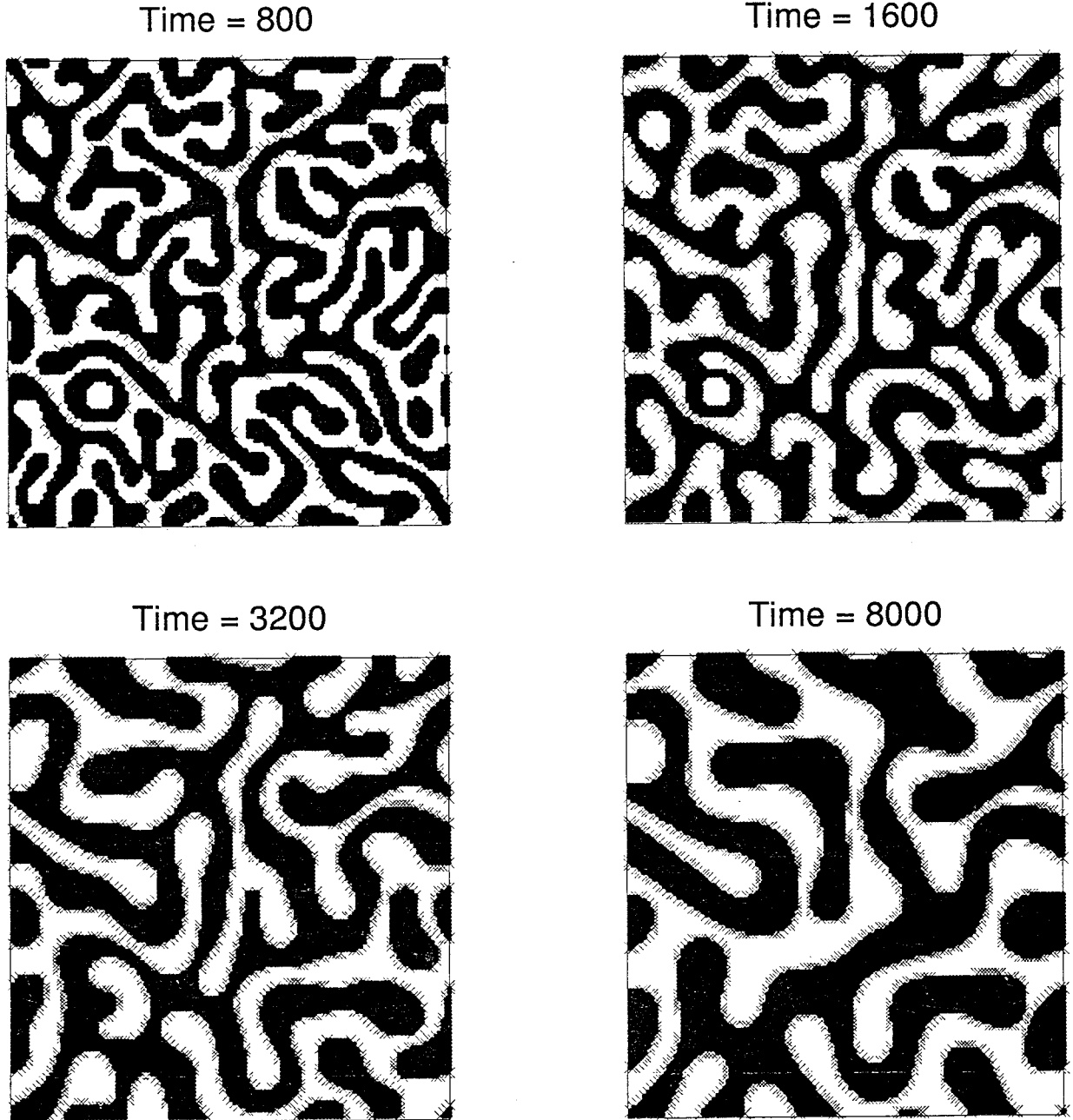


FIG. 1. Evolution pictures of vacancy-mediated phase separation in an ABV model, obtained from a simulation of our mean-field (MF) dynamical model in Eqs. (3) and (4). The lattice size was 128^2 and periodic boundary conditions were applied in both directions. Parameter values and the initial conditions for our simulation are described in the text. Regions with positive $\langle S_k \rangle$ (A -rich) are marked in black and regions with negative $\langle S_k \rangle$ (B -rich) are unmarked. Regions where $\langle S_k^2 \rangle$ falls below 0.7 (V -rich) are marked by crosses and are confined to the interfacial regions. The dimensionless times corresponding to the pictures are specified above each frame.

atom. We assume that there is only a nearest-neighbor interaction (denoted by ϵ_{ij} , where $i, j \equiv A$ or B or V); and that there is no interaction energy associated with a pair containing at least one V atom. Then, we can write the energy of this system in terms of a spin-1 model as

$$H = -J \sum_{\langle ij \rangle} S_i S_j + K \sum_{\langle ij \rangle} S_i^2 S_j^2, \quad (1)$$

where J and K depend in a simple fashion on ϵ_{ij} 's and we have assumed that $\epsilon_{AA} = \epsilon_{BB} (< 0)$, so that there is an attrac-

tive interaction between like atoms. The spin states $S_i = +1, 0$ and -1 refer to the site i being occupied by A, V and B , respectively. The Hamiltonian in (1) is well known as the Blume-Emery-Griffiths model [10] and we will investigate phase ordering dynamics in this model.

We associate stochastic dynamics with this model by allowing for only $A \leftrightarrow V$ ($1 \leftrightarrow 0$) and $B \leftrightarrow V$ ($-1 \leftrightarrow 0$) nearest-neighbor exchanges. The master equation which describes the evolution of the probability distribution function $P(\{S_i\}; t)$ for a spin configuration $\{S_i\} (i=1 \rightarrow N)$ is as follows:

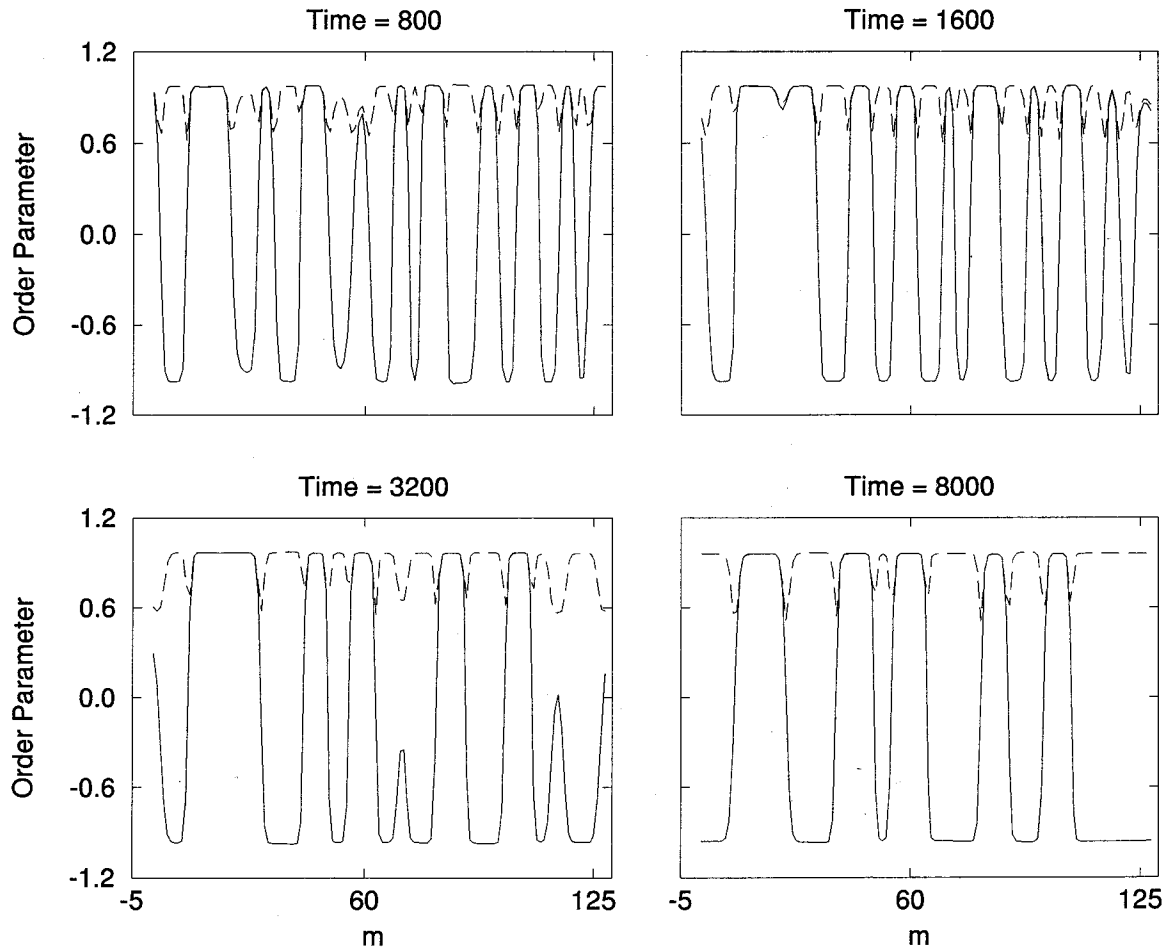


FIG. 2. Order parameter profiles along a cross section in the frames of Fig. 1. The profiles are measured along a horizontal cross section, located at the middle of the vertical axis. The $\langle S_k \rangle$ (or AB) field is denoted by a solid line; and the $\langle S_k^2 \rangle$ (or V) field is denoted by a dashed line.

$$\begin{aligned}
 & \frac{\partial}{\partial t} P(S_1, \dots, S_i, S_{L_i}, \dots, S_N; t) \\
 &= - \sum_i \sum_{L_i} W(S_i \leftrightarrow S_{L_i}) [1 + S_i S_{L_i}] \\
 & \quad \times P(S_1, \dots, S_i, S_{L_i}, \dots, S_N; t) \\
 & \quad + \sum_i \sum_{L_i} W(S_{L_i} \leftrightarrow S_i) [1 + S_i S_{L_i}] \\
 & \quad \times P(S_1, \dots, S_{L_i}, S_i, \dots, S_N; t). \quad (2)
 \end{aligned}$$

In Eq. (2), the notation L_i refers to neighbors of i . The first and second terms on the right-hand side (RHS) account for transitions out of and into the configuration $\{S_i\}$, respectively. The functional form of the transition probability $W(S_i \leftrightarrow S_{L_i})$ is chosen to satisfy the usual detailed balance condition [3,11] and the factor $[1 + S_i S_{L_i}]$ enforces the constraint that only $\pm 1 \leftrightarrow 0$ exchanges are allowed.

Here, we will only describe the procedure we follow to obtain our MF dynamical models. Details of the derivation will be presented elsewhere [11]. In the present problem, we have two order parameters, $\langle S_k \rangle$ (which refers to the AB field); and $\langle S_k^2 \rangle$ (which refers to the V field). We obtain

dynamical equations for these quantities by multiplying Eq. (2) by S_k or S_k^2 and averaging over all initial configurations. The resultant equations are exact but intractable. These equations are simplified using the MF approximation. The resultant dynamical model for the case $K=0$ is as follows [11]:

$$\begin{aligned}
 \frac{\partial \langle S_k \rangle}{\partial t} &= -q \langle S_k \rangle + \sum_{L_k} \langle S_{L_k} \rangle - \sum_{L_k} (\langle S_k^2 \rangle \langle S_{L_k} \rangle - \langle S_k \rangle \langle S_{L_k}^2 \rangle) \\
 & \quad + \sum_{L_k} (\langle S_k^2 \rangle + \langle S_{L_k}^2 \rangle - 2 \langle S_k \rangle \langle S_{L_k} \rangle) \\
 & \quad \times \tanh \left[\frac{J}{2T} \left(\sum_{L_k} \langle S_{L_k} \rangle - \sum_{L_{L_k}} \langle S_{L_{L_k}} \rangle \right) \right], \quad (3)
 \end{aligned}$$

and

$$\begin{aligned}
 \frac{\partial \langle S_k^2 \rangle}{\partial t} &= -q \langle S_k^2 \rangle + \sum_{L_k} \langle S_{L_k}^2 \rangle \\
 & \quad + \sum_{L_k} (\langle S_k \rangle + \langle S_{L_k} \rangle - \langle S_k \rangle \langle S_{L_k}^2 \rangle - \langle S_k^2 \rangle \langle S_{L_k} \rangle) \\
 & \quad \times \tanh \left[\frac{J}{2T} \left(\sum_{L_k} \langle S_{L_k} \rangle - \sum_{L_{L_k}} \langle S_{L_{L_k}} \rangle \right) \right], \quad (4)
 \end{aligned}$$

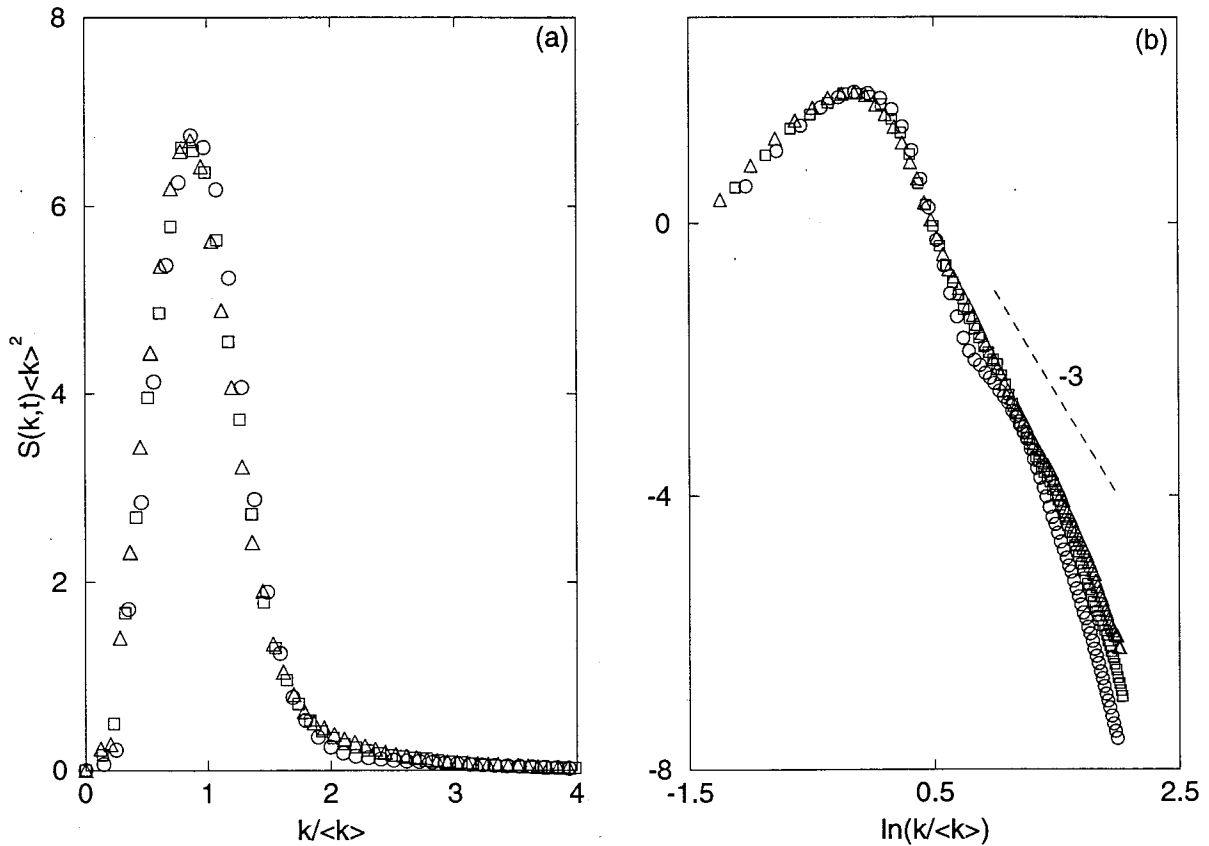


FIG. 3. (a) Comparison of scaled structure factors $S(k,t)\langle k \rangle^2$ vs $k/\langle k \rangle$ for vacancy-mediated phase separation with $v_0=0.93$ (denoted by \square 's) and $v_0=0.96$ (denoted by \triangle 's); and the usual Kawasaki-exchange or pure case (denoted by \circ 's). All structure factor data is obtained on systems of size 256^2 as an average over 50 independent runs. Data for the vacancy-driven and pure cases is at dimensionless times 8000 and 4000, respectively. (b) Log-log plot of the data from (a). Symbols have the same meaning as in (a). The dashed line refers to the two-dimensional version of Porod's law, i.e., $S(k,t) \sim k^{-3}$.

where q is the number of nearest neighbors for a site; and T is the temperature ($k_B=1$). Equations (3) and (4) constitute our MF dynamical model for vacancy-mediated phase separation for $K=0$. We have confirmed that Eqs. (3) and (4) contain the correct MF static solution [11], an essential check on the reasonableness of the model. We can also obtain the equivalent nonlinear partial differential equation model by identifying $\langle S_k \rangle \equiv \psi(\vec{r}, t)$ and $\langle S_k^2 \rangle \equiv \phi(\vec{r}, t)$ and Taylor-expanding the terms on the RHS of Eqs. (3) and (4) [11]. However, our numerical results are obtained by directly simulating Eqs. (3) and (4) and, therefore, we will not present the nonlinear partial differential equation model here. Finally, we have also obtained a general model for $K \neq 0$ and will present it elsewhere [11].

We have used the MF dynamical model in Eqs. (3) and (4) to simulate vacancy-mediated phase separation. We used a simple Euler discretization scheme with mesh size $\Delta t=0.01$ on a two-dimensional lattice of size N^2 . In general, the Euler discretization scheme used by us is numerically inaccurate unless very small mesh sizes are used. However, phase ordering systems are strongly driven towards a stable fixed point and this gives rise to a dynamical universality, i.e., quantitatively similar results are obtained for statistically relevant quantities from both the continuum models and their Euler-discretized versions even if the discretization mesh sizes are rather large [9,12]. (Of course, the mesh sizes must

not be such that the numerical scheme becomes unstable.) We have confirmed that the numerical results presented below are unchanged on further reduction of the mesh size Δt . Periodic boundary conditions were applied in both directions of the lattice. The parameter value for our simulation was $T=0.375T_c$, where $T_c(=2qJ/3)$ is the MF critical temperature for our model.

The initial conditions for the $\langle S_k \rangle$ and $\langle S_k^2 \rangle$ fields consisted of uniformly distributed random fluctuations about a background value; and mimicked the disordered homogeneous state prior to the quench. The background value for the $\langle S_k \rangle$ field was 0, corresponding to an equal number of A and B atoms. For the $\langle S_k^2 \rangle$ field, we considered background values $v_0=0.93$ and 0.96 , which corresponds to a fairly high concentration of vacancies. We worked with these high vacancy concentrations as we were interested in nonuniversal effects which may arise because of the presence of vacancies.

Figure 1 shows the temporal evolution of our model with $v_0=0.96$. These pictures were obtained on a lattice of size 128^2 . Regions where $\langle S_k \rangle$ is positive (say, A -rich) are marked in black and regions where $\langle S_k \rangle$ is negative (B -rich) are unmarked. We define vacancy-rich regions as being those where $\langle S_k^2 \rangle$ falls below 0.7 and these are marked by crosses in Fig. 1. It is evident that the vacancies rapidly

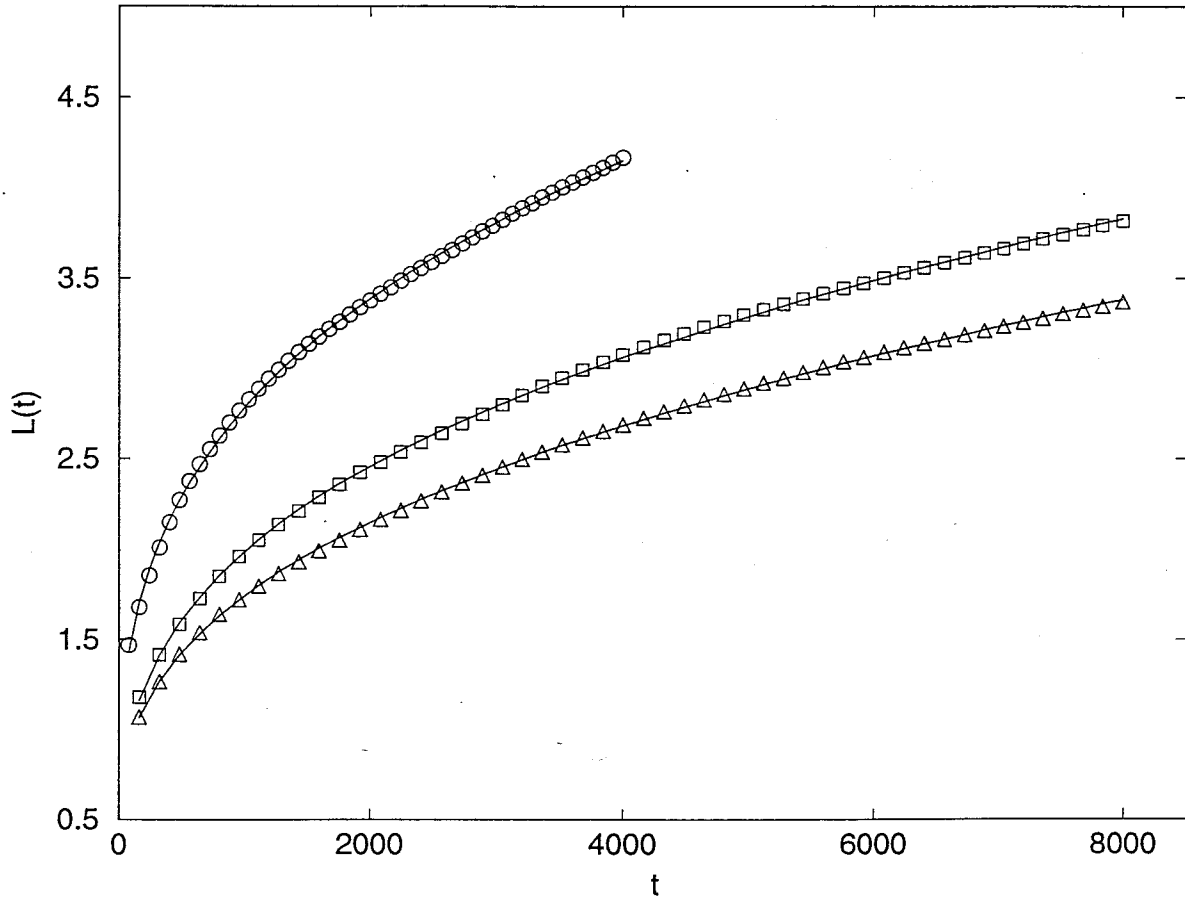


FIG. 4. Time-dependence of the characteristic length scale $L(t)$ vs t for vacancy-mediated phase separation. We present data for $v_0=0.93$ (denoted by \square 's) and $v_0=0.96$ (denoted by \triangle 's). For purposes of comparison, we also present data for the pure case (denoted by \circ 's). We fit the data to the form $L(t)=a+bt^\phi$ using a nonlinear fitting routine. The resultant best-fits are denoted as solid lines on the appropriate data sets. The best-fit exponents are $\phi=0.33\pm 0.01$ for the pure case; $\phi=0.34\pm 0.01$ for $v_0=0.93$; and $\phi=0.32\pm 0.01$ for $v_0=0.96$.

migrate to the interfacial regions. This is clarified further in Fig. 2, where we plot the order parameter profiles along a cross section of the frames in Fig. 1. The solid and dashed lines refer to the $\langle S_k \rangle$ and $\langle S_k^2 \rangle$ fields, respectively. The dips in the $\langle S_k^2 \rangle$ profile (i.e., V -rich regions) are coincident with the zero-crossings of the $\langle S_k \rangle$ profile (i.e., interfacial regions between A - and B -rich domains).

We have also investigated the scaling behavior of the time-dependent structure factor of the $\langle S_k \rangle$ field. This experimentally relevant quantity is calculated on systems of size 256^2 as an average over 50 independent runs. We spherically average the resultant structure factor $S(\vec{k}, t)$ to get the scalarized structure factor $S(k, t)$, which we will present subsequently. Furthermore, the characteristic domain length scale $L(t)$ is defined as the reciprocal of the first moment $\langle k \rangle$ of the scalarized structure factor, i.e., $L(t) = \langle k \rangle^{-1}$.

We have confirmed that the structure factor $S(k, t)$ corresponding to the evolution depicted in Fig. 1 exhibits dynamical scaling. For the sake of brevity, we will not show these results here. Rather, Fig. 3 compares the scaled structure factor for vacancy-driven segregation with that for the usual Kawasaki-exchange kinetics in the binary alloy AB . The data for the Kawasaki-exchange case is obtained using the appropriate MF dynamical model with system sizes and statistics

similar to those described previously. Figure 3(a) compares scaled structure factors for the vacancy-driven case with $v_0=0.93$ and 0.96 (denoted by \square 's and \triangle 's, respectively); and that for Kawasaki-exchange kinetics, referred to as the pure case and denoted by \circ 's. The scaled structure factors agree reasonably well on this scale, with a slight discrepancy for $k/\langle k \rangle \geq 2$. This discrepancy is highlighted in Fig. 3(b), which is a log-log plot of the data in Fig. 3(a). The shoulder in the data for the pure case at $k/\langle k \rangle \approx 2$ is missing in the vacancy-driven case. This is a possible consequence of the slow approach to asymptotia in our vacancy-driven model. There are also discrepancies in the extreme tail region, which we discuss briefly here. None of the scaled structure factors exhibit the Porod tail [$S(k, t) \sim k^{-(d+1)}$ for large k], which characterizes scattering off sharp interfaces. In the pure case, this is understood to be a consequence of the finite interfacial thickness σ_w and it is expected that the Porod tail will appear in the limit $\sigma_w/L(t) \rightarrow 0$ [13]. However, in the vacancy-driven case, there is an ongoing accretion of vacancies in the interfacial regions. This gives a time dependence to the interface thickness and it is possible that the scaled data never exhibits a Porod tail [14]. We will elaborate this point elsewhere [11].

Finally, Fig. 4 shows the time dependence of the charac-

teristic length scale $L(t)$. We plot $L(t)$ vs t for the vacancy-driven cases with $v_0=0.93$ and 0.96 ; and the pure case. We have used a nonlinear fitting routine to fit data to the form $L(t)=a+bt^\phi$ and the resultant best-fits are superposed on the data sets. The best-fit exponents are specified in the figure caption and are all consistent with the Lifshitz-Slyozov growth law $L(t)\sim a+bt^{1/3}$. Of course, the ongoing deposition of vacancies in the interfacial regions gives a weak time dependence to the surface tension, which should finally result in a slowing down of the domain growth [14]. However, we have not accessed this extreme late-stage behavior in our simulations as yet.

Let us end this paper with a brief summary and discussion of our results. We have formulated a MF dynamical model for vacancy-mediated phase separation in ABV mixtures. Our approach is general and can easily be extended to arbitrary ternary mixtures. We believe that such models will prove very useful in investigating the asymptotic behavior of

phase ordering in ternary mixtures. We have also presented numerical results from our MF model, which demonstrate that the growth exponent for vacancy-mediated phase separation is consistent with the Lifshitz-Slyozov growth law over the time scales of our simulation. Furthermore, the scaled structure factor for vacancy-mediated phase separation is similar to that for the usual Kawasaki-exchange case, except for differences in the tail region. Our results support the view that vacancy-mediated segregation and phase separation via Kawasaki-exchange kinetics are in the same dynamical universality class over extended time scales.

The author is grateful to K. Binder for suggesting this problem and for many useful discussions. He would also like to thank S. Dattagupta, A.J. Bray, P. Fratzl, J.L. Lebowitz, Y. Oono and O. Penrose for useful inputs. Finally, he is grateful to Y. Oono and A.J. Bray for inviting him to Urbana and Manchester, respectively, where most of the numerical results described in this paper were obtained.

-
- [1] For reviews, see J.D. Gunton, M. San Miguel, and P.S. Sahni, in *Phase Transitions and Critical Phenomena*, edited by C. Domb and J.L. Lebowitz (Academic Press, New York, 1983), Vol. 8, p. 267; K. Binder, in *Materials Science and Technology, Vol. 5: Phase Transformations of Materials*, edited by R.W. Cahn, P. Haasen, and E.J. Kramer (VCH, Weinheim, 1991), p. 405; A.J. Bray, *Adv. Phys.* **43**, 357 (1994).
- [2] K. Binder and D. Stauffer, *Phys. Rev. Lett.* **33**, 1006 (1974); *Z. Phys. B* **24**, 406 (1976).
- [3] K. Kawasaki, in *Phase Transitions and Critical Phenomena*, edited by C. Domb and M.S. Green (Academic Press, New York, 1972), Vol. 2, p. 443; and references therein.
- [4] J.R. Manning, *Diffusion Kinetics for Atoms in Crystals* (Van Nostrand, Princeton, 1968); C.P. Flynn, *Point Defects and Diffusion* (Clarendon, Oxford, 1972).
- [5] K. Yaldram and K. Binder, *Acta Metall.* **39**, 707 (1991); *Z. Phys. B* **82**, 405 (1991); *J. Stat. Phys.* **62**, 161 (1991).
- [6] P. Fratzl and O. Penrose, *Phys. Rev. B* **50**, 3447 (1994).
- [7] J.G. Amar, F.E. Sullivan, and R.D. Mountain, *Phys. Rev. B* **37**, 196 (1988).
- [8] K. Binder, *Z. Phys. B* **267**, 313 (1974); K. Binder and H.L. Frisch, *ibid.* **84**, 403 (1991).
- [9] Y. Oono and S. Puri, *Phys. Rev. Lett.* **58**, 836 (1987); *Phys. Rev. A* **38**, 434 (1988); S. Puri and Y. Oono, *ibid.* **38**, 1542 (1988); *J. Phys. A* **21**, L755 (1988); A. Chakrabarti and J.D. Gunton, *Phys. Rev. B* **37**, 3798 (1988).
- [10] M. Blume, V.J. Emery, and R.B. Griffiths, *Phys. Rev. A* **4**, 1071 (1971); D. Furman, S. Dattagupta, and R.B. Griffiths, *Phys. Rev. B* **15**, 441 (1977).
- [11] S. Puri and R. Sharma (unpublished).
- [12] T.M. Rogers, K.R. Elder, and R.C. Desai, *Phys. Rev. B* **37**, 9638 (1988).
- [13] Y. Oono and S. Puri, *Mod. Phys. Lett. B* **2**, 861 (1988).
- [14] R. Ahluwalia and S. Puri, *J. Phys. Condens. Matter* **8**, 227 (1996).